

Modeling Interactive Receptive Fields in Sensory Systems

**Abraham Akinin
Cory Stevenson**

**BENG 260 Project
Department of Bioengineering UCSD**

Abstract

An integrate-and-fire model of a one dimensional cellular neural network was developed to assess the effects of receptive field interconnectivity on image processing. Using this model it was found that negative inhibition of neighboring fields pronounced the edges of areas of activation, and was linearly dependent on the strength of the connection, the magnitude of the inputs, and spatial frequency of inputs. Similar effects were seen in second neighbor interactions, however with a non-linear relationship in the magnitude dependence and no relation for frequency dependence.

1 Introduction

1.1 Nature of Sensory Systems

Receptive fields are present in many sensory systems, including the visual and somatosensory systems. In the visual system ganglion cells receive signals originating from photoreceptors within their receptive field [1]. The nature of the receptive fields help dictate the resulting perception of a stimulus interpreted through the sensory system. The size and density of the receptive field determine the spatial resolution of the sensory system; large fields provide high sensitivity, but low resolution, with the opposite true for smaller receptive fields [2]. In the retina, the fovea, possesses smaller receptive fields for the ganglion cells, synapsing with color photoreceptors, leading to a high spatial acuity, as compared to the larger, less dense receptive fields in the peripheral retina composing primarily of rod photoreceptors [3].

The interaction of neurons within and between receptive fields additionally affects the perceptions of stimuli. Inhibitory and excitatory affects from the periphery of the receptive field are used to change the response to specific stimulation. One example of this being the center-surround interaction in the fovea, where stimulation at the center of the receptive field induces activation and the surrounding induces inhibition, or the reverse [1]. In addition to this spatial functionality, there is evidence for sensitivity to the stimulus type, such as color, being used in conjunction with center-surround interactions [1]. This leads to the result that stimuli within the receptive field are responded to differentially, based on their position relative to the center of the receptive field and nature of the stimulus. This has effects such as edge sharpening, where the interaction of neighboring locations yields an exaggeration of differences between neighboring locations, hence enhancing "edges" which were presented in the stimulus [4]. This process for edge detection has been compared to using a Gabor filter in computerized visual processing, and has led to its use in modeling of the visual system [5].

1.2 Previous Modeling

The integrate-and-fire neuron model is commonly used to simulate interacting neurons in sensory systems. In the integrate-and-fire model each neuron is modeled as a non leaking capacitor[6].

$$C \frac{dV_n}{dt} = \sum I$$

Each neuron integrates all inputs until its voltage reaches a threshold, the neuron then discharges an action potential and enters into a refractory period. This model is often used for modeling cellular neural networks, as it simplifies the representation and computational load necessary to model a single neuron, while retaining effects of the neuron firing and behavior in interacting with its neighbors [7]. This general model has been used to model many neural networks and variations have been made to improve its accuracy, such as the leaky integrate-and-fire model, which addresses the temporal aspect of input summation [6].

1.3 Objectives

The goal of this project is to implement an integrate-and-fire model to portray interconnected receptive fields in a sensory system. This model will then be used to assess the interaction of neighboring receptive fields with varying interconnectivities on the resulting perception of presented stimuli.

2 Methods

2.1 Implementation

The implemented integrate-and-fire model for cellular neuronal networks simulates a one dimensional network of 100 ganglion cells. A 1-D “picture” of activations is presented to the network, simulated by direct injection of a constant current. At each timestep this current is added to the cell increasing the membrane potential. Additionally, currents from the action potentials of neighboring cells can either inhibit or excite the cell by injecting negative or positive currents.

$$V[n]_t = V[n]_{t-1} + \frac{I_{in}[n]}{C} * dt + \sum_{i=\pm 1, 2, \dots} T[n+i]_{t-1} * C[i]$$

In the above equation $V[n]$ represents the membrane potential of the n^{th} cell. $I[n]$ is the injected current from the stimulus, and C and dt are the membrane capacitance and the timestep of the system. T is a binary variable that is ‘1’ when neuron at ‘ $n+1$ ’ reached or surpassed a reference voltage in the previous timestep. When the membrane potential reaches or surpasses a critical threshold potential (20 mV above the resting potential in our simulation) the neuron generates an action potential. The action potential is logged and the cell enters a refractory period, where it cannot fire (this period lasts 20 ms in our simulation) and during which the cell does not integrate any input. When the refractory period is over the cell begins to integrate the injected current starting from the resting potential, repeating the cycle. When the simulation is run, the number of action potentials for a particular cell are counted and an average firing rate is calculated based on the run time; this rate is used to quantitatively approximate the output that would be perceived downstream for a system using this sensory model.

2.2 Model Development

The basic structure of the model described above was implemented to generate a working model. In order to make the model functional, some additional functionalities were introduced. One requirement was the initialization of each cell membrane voltage to a randomized sub-threshold value. This was necessary to introduce an initial stochastic desynchronization element so that all of the cells did not start off at the same potential; if this were not implemented then cells receiving an activating input would have simultaneous action potentials followed by simultaneous refractory periods, therefore not allowing the cells to be affected by the neighboring potentials.

To inject the current into the cells, the stimulus was a 1-D vector with values between 0 and 1; 0 for no activation, 1 for full activation. For experimental purposes of model characterization only ‘on’ and ‘off’ stimuli were used. These stimuli and the magnitude of the

synaptic interactions were scaled. Determination of the scaling factor is part of the characterization of the model.

From this basic model of injected stimulus and neighboring currents two regimes were developed. The first regime was individual cells connected to their immediate neighbors using inhibitory currents. The second regime was expanding the first into a next-next neighbor model, where the immediate neighbor was inhibited by a cell and the next neighbor was excited by the cell, but to a smaller degree.

3 Results

After the model was developed, simulations were run changing the parameters and analyzing the behavior. With no interconnectivity between neurons, the output spike frequency, of a particular neuron matched spatially with the input “image”: where there was an input, spiking occurred. However, because of the introduction of initial noise where there was a non-zero activation there were small stochastic variations in spiking frequency across the activated area that varied across experimental trials.

When connection strength between cells was non-zero edge effects occurred. The connectivity between neurons was reported as relative connectivity; assessed as the voltage caused by the activation of that connection with respect to its percentage of the threshold potential. When the connectivity strength was providing an inhibitory input the edge effect was a pronunciation of the edge of an activating area. The spiking frequency of the neurons at the edge of the image increased above the neurons in the center, by providing negative inhibition. The magnitude of this effect, the edge-effect ratio (EER), was calculated as the ratio of the average spiking frequency at the edges of an activated area to the average spiking frequency within the activated area. This was one of the primary effects used to measure the behavior of the system. When the connectivity strength was excitatory the edges of the activating block became less pronounced. The higher the connection strength the larger the spread of the edge signal, as a cell is activated it increases the activation of its neighbors, which in turn activate their neighbors, spreading the signal to other non-excited neurons.

3.1 First Regime: Immediate Neighbor Connections Only

As the connection strength was varied the pronunciation of the edge was affected. Stronger inhibitory connection strength increased the EER for a particular input signal as seen in the linear relationship in Figure 1. For values higher than 0.5 the neurons began to synchronize and stopped creating edge effects.

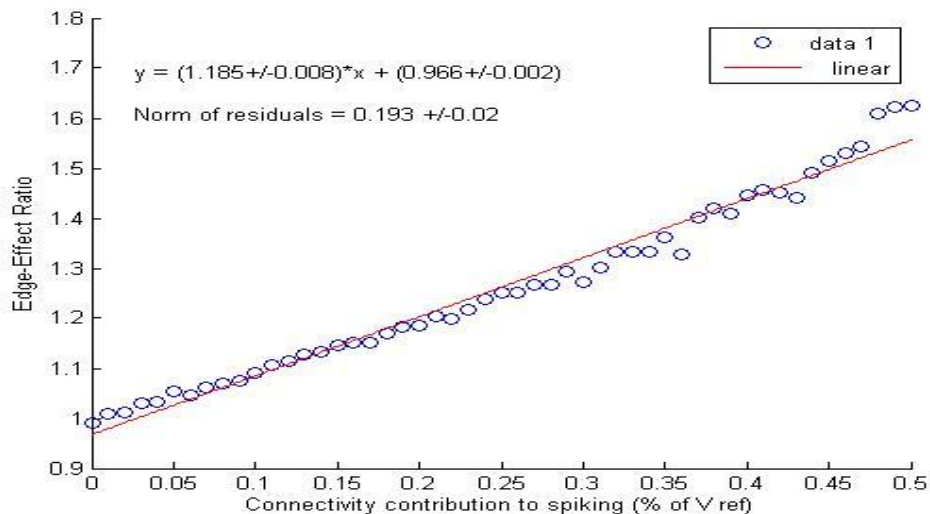


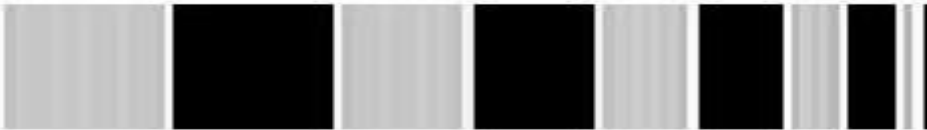
Figure 1: The effect of relative connectivity between neighbors on EER. Higher connectivity contribution corresponds to stronger inhibitory connections.

$$\text{Connectivity Contribution to spiking} = \frac{\Delta V}{V_{\text{ref}}} \text{ caused by a single action potential}$$

In addition to varying with connectivity, the spatial resolution of the model affects edge pronunciation. The spatial resolution of the model can be seen in Figure 2, which shows the output of the network in response to a binary chirp along the spatial domain, starting with an input of 19 units on, 17 off, and so forth. The response with no interconnectivity produces a nearly identical output to the input signal with no enhancement of the edge. With a -25% connectivity the pronunciation of the edges can be seen (as brighter bands) in blocks of activation. The magnitude of this effect is further affected by the spatial frequency of the input. This effect is based upon the spatial frequency and interaction between adjoining cells. As the spatial frequency of the input increases, the EER increases linearly, as seen in Figure 3. The larger blocks become, the less pronounced the effect on EER is. This effect is primarily from the interaction of neurons close to each other. On either side of the block there is a strongly activated neuron, inhibiting all the local neurons; with a small block the nearby neurons are inhibited from both sides, making for a lower feedback control and a higher firing rate at the edges.



Figure 2: (Top) The output results of a binary spatial chirp with no interconnectivity between cells. (Bottom). Response to the same input with a -25%



connectivity contribution by synapses. Notice some very small variation in the white areas of the top figure as a result of the random initialization of the neurons. Each image was independently normalized to make the maximum value white and 0 as black

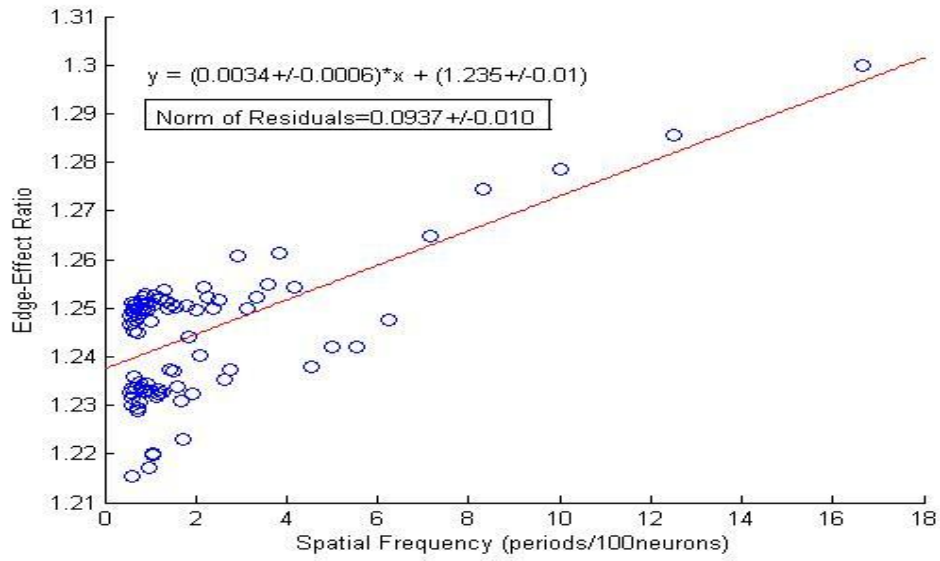


Figure 3: The effects of spatial frequency on EER. Connectivity contribution to spiking is fixed at -25% while theta is fixed at 0.1.

Another defining characteristic of our model was the effect of the control factor, θ , on system. Theta was defined as the ratio of the refractory period of the system to the complete period of one neuron's oscillation as a function of the input current magnitude when there is no synaptic connectivity.

$$\theta = \frac{t_{ref}}{t_{ref} + \frac{C * V_{ref}}{I_{Magnitude} * dt}}$$

. Since the length of the refractory period, capacitance, and the threshold membrane potential were held fixed, the quotient between the threshold potential and the total amount of injected current at each timestep dictates the number of timesteps necessary to reach the threshold potential. Theta is thus a non-dimensionalized variable that increases monotonically with stimulation magnitude and accurately represents the proportion of time that neurons are deaf to synaptic and stimulative inputs.

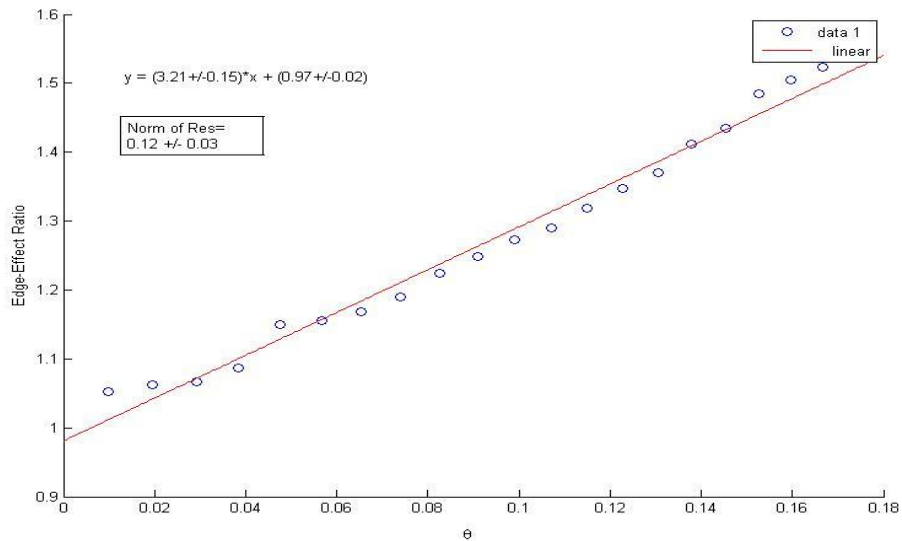


Figure 4: The effects of theta adjustment on EER.

The value of theta has some important consequences on the model. First of all theta cannot be above a level where the neurons fire immediately; the input currents generate thresholds so high that they spike immediately after exiting the resting potential. In this case the firing rate of the system is then not controlled by the inputs received during the integrating period, but by the fixed length of the refractory period. Therefore the dynamic nature of the model is lost. Secondly, as seen in Figure 4, as theta increases the EER of the system increases, even with the relative connectivity of the cell connections remaining constant (-25% in figure 4). This is due to the fact that the edge cells fire more frequently than their neighbors because they are only inhibited by one neighbor, as the rate at which they reach the threshold potential has increased, making the difference in magnitude between the edge and the center of the activation area more pronounced. This last graph also depicts how this system is different from other image processing systems that do not have magnitude dependent deviations. For theta values greater than 20% edge effects were lost to noise amplification and periodic oscillations.

The fittings and std. dev. in figures 1,3 and 4 are an accrument of 10 identical experiments to show that the random initialization does not have a significant impact on the model.

When the refractive period becomes more than 20% of the neuron's cycle the linear relation observed in figure 4 disappears for a chaotic pattern that aside from not detecting edges is very volatile for different random initialization values.

3.2 Second Regime: Next Neighbor Connections

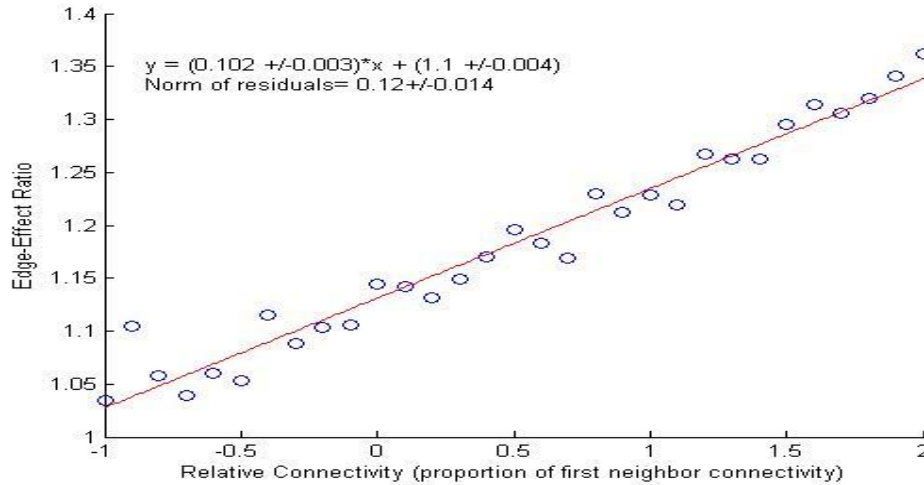


Figure 5. The effect of the relative values of second neighbor connectivity with respect to the first neighbor for 0.25 connectivity contribution of first neighbor. At '-1' the edge effect almost disappears because the inhibition created by next neighbors is being counteracted by excitation from next-next-neighbors while at '1' there is double inhibition: from next neighbors and next-next neighbors.

In figure 5 we can see that second neighbor acts as an amplifier or suppressor of what the first neighbor does.

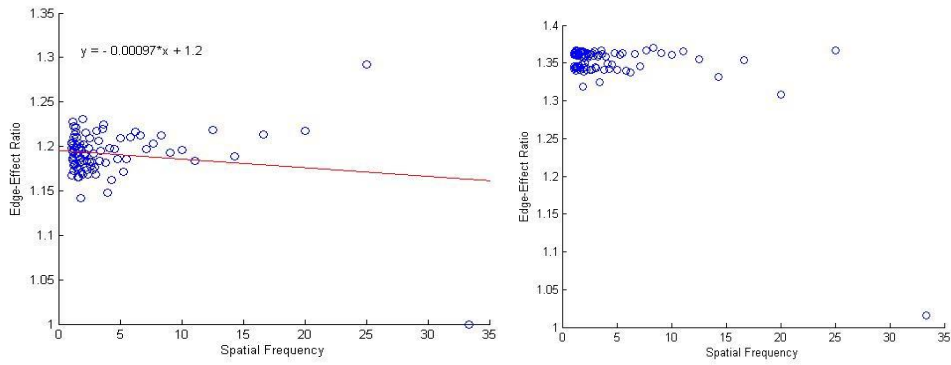


Figure 6. The effect of spatial frequency on EER as a function of frequency for relative connectivity -0.5 (LEFT) and 0.5 (RIGHT). Notice the effect of relative connectivity as described in figure 5 and the fact that in between these two regimes there is Figure 3.

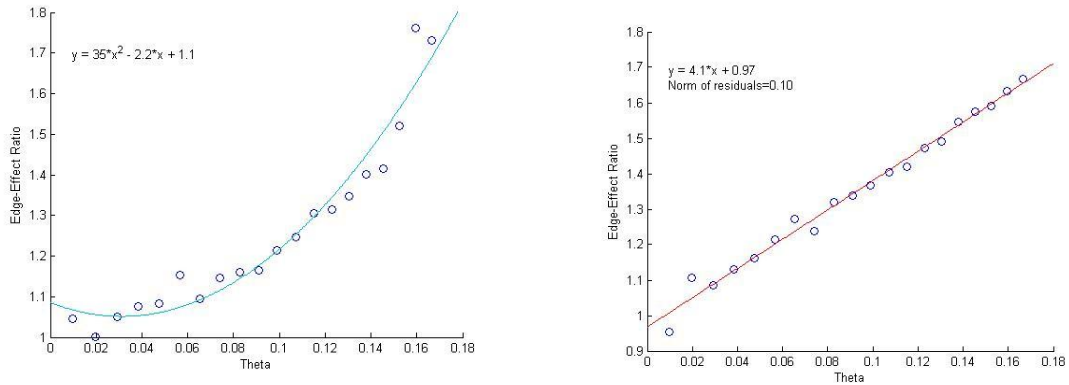


Figure 7. The effect of magnitude (or theta) on the EER for -0.5 and 0.5 relative connectivities.

Notice that as the second neighbor becomes more opposite to the first, the linear relationship between theta and EER is transformed into a quadratic like curve. When they are both the same sign the graph is linear but with a higher slope than figure 4.

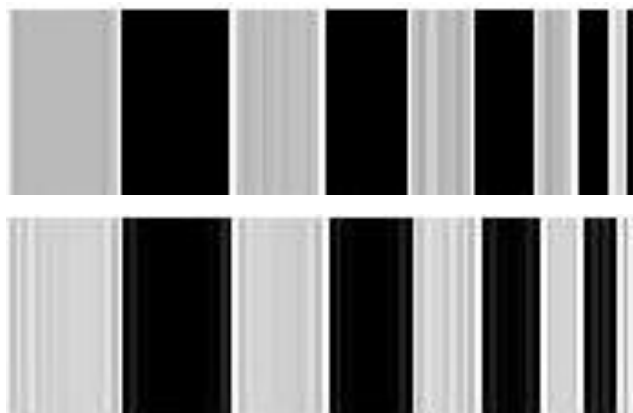


Figure 8. The output of the system to an input chirp as described above with double neighbor interactions. (TOP) has positive second neighbor relative connectivity (inhibiting-inhibiting) while (BOTTOM) has negative relative connectivity (inhibiting excitatory). The bottom graph shows noise in the silent (black) part of the input and though EER is lower notice the edges are just as highlighted in the higher frequency range (right part of the image)

4 Conclusions

In this project we modeled what might be the basis for the action of neurosensory systems to condition signals for further processing in the central nervous system. Edge detection and lateral inhibition are important functions of local receptive fields that enable the central nervous system to discriminate between inputs. In organizing the project we analyzed all the parameters in terms of non dimensional variables that should extend to other types of models for arbitrary number of neurons, or reference voltage or refractory period to universally describe the system .

We observed that these systems can codify spatial and intensity differences based on the system parameters for a range of conditions and outside that range they are not able to do so as well. Frequency dependent edge magnification falls apart when most of the cells are in the refractory period all the time. This suggests that we might not be as accurate in identifying the contours of very bright object which is indeed what happens. Second neighbor interactions turn out to completely eliminate frequency dependent EER. Also, as expected, second neighbor interactions themselves have an effect on the magnitude of EER in a similar way than the first neighbor connectivity does.

4.1 Future Directions

The next major step to expand the functionality of the model consists of extending the 1-D model, which shows proof of concept of cellular interactions, to a two dimensional model. This will allow the model stimulation to be in the form of two dimensional “images”, such as perceived by biological senses of touch and vision and show that the model can emulate many “optical illusions”.

The model could also be improved by changing the basic equations to the leaky-integrate-and-fire model. This would allow for temporal aspects of the model, as membrane potentials would not integrate indefinitely till passing threshold, they would decay if more input was not given. This temporal nature would allow for dynamic, time-variant inputs to the model.

Another improvement for the model is by improving the patterns of connectivity, where the cells connect with cells in their vicinity, but not necessarily their immediate neighbors. Additionally, each cell would be given a range of connection strengths, so that the various connections would each be a different value. One effect of this is to better model a biological system where neurons do not necessarily synapse with their immediate neighbors or with the same strength. This would also possibly allow for the addition of learning functionalities where connection strengths are increased.

5 References

- [1] Weber, C., Triesch, J.; “Implementations and Implications of Foveated Vision,” *Recent Patents on Computer Science*, 2, 75-85, 2009
- [2] Johansson, R.S.; “Tactile sensibility in the human hand: receptive field characteristics of mechanoreceptive units in the glabrous skin area”. *J Physiol* 281: 101–123, 1978.
- [3] XuDong Guan; Hui Wei; , "Realistic Simulation on Retina Photoreceptor Layer," *Artificial Intelligence, 2009. JCAI '09. International Joint Conference on* , vol., no., pp.179-184, 25-26 April 2009
- [4] Chao-Hui Huang; Chin-Teng Lin; , "Bio-Inspired Computer Fovea Model Based on Hexagonal-Type Cellular Neural Network," *Circuits and Systems I: Regular Papers, IEEE Transactions on* , vol.54, no.1, pp.35-47, Jan. 2007
- [5] Shi, B.E.; , "Gabor-type filtering in space and time with cellular neural networks," *Circuits and Systems I: Fundamental Theory and Applications, IEEE Transactions on* , vol.45, no.2, pp.121-132, Feb 1998

- [6] Hansel D, Mato G, Meunier C, and Neltner L. "On numerical simulations of integrate-and-fire neural networks". *Neural Comput* 10: 467–483, 1998.
- [7] Serbedzija, N.B.; , "Simulating artificial neural networks on parallel architectures," *Computer* , vol.29, no.3, pp.56-63, Mar 1996
- [8] Balasuriya, S.; Siebert, P.; , "A biologically inspired computational vision front-end based on a self-organised pseudo-randomly tessellated artificial retina," *Neural Networks, 2005. IJCNN '05. Proceedings. 2005 IEEE International Joint Conference on* , vol.5, no., pp. 3069- 3074 vol. 5, 31 July-4 Aug. 2005